

LETTERS

Improved estimates of upper-ocean warming and multi-decadal sea-level rise

Catia M. Domingues¹, John A. Church^{1,2}, Neil J. White^{1,2}, Peter J. Gleckler³, Susan E. Wijffels¹, Paul M. Barker¹ & Jeff R. Dunn¹

Changes in the climate system's energy budget are predominantly revealed in ocean temperatures^{1,2} and the associated thermal expansion contribution to sea-level rise². Climate models, however, do not reproduce the large decadal variability in globally averaged ocean heat content inferred from the sparse observational database^{3,4}, even when volcanic and other variable climate forcings are included. The sum of the observed contributions has also not adequately explained the overall multi-decadal rise². Here we report improved estimates of near-global ocean heat content and thermal expansion for the upper 300 m and 700 m of the ocean for 1950–2003, using statistical techniques that allow for sparse data coverage^{5–7} and applying recent corrections⁸ to reduce systematic biases in the most common ocean temperature observations⁹. Our ocean warming and thermal expansion trends for 1961–2003 are about 50 per cent larger than earlier estimates but about 40 per cent smaller for 1993–2003, which is consistent with the recognition that previously estimated rates for the 1990s had a positive bias as a result of instrumental errors^{8–10}. On average, the decadal variability of the climate models with volcanic forcing now agrees approximately with the observations, but the modelled multi-decadal trends are smaller than observed. We add our observational estimate of upper-ocean thermal expansion to other contributions to sea-level rise and find that the sum of contributions from 1961 to 2003 is about $1.5 \pm 0.4 \text{ mm yr}^{-1}$, in good agreement with our updated estimate of near-global mean sea-level rise (using techniques established in earlier studies^{6,7}) of $1.6 \pm 0.2 \text{ mm yr}^{-1}$.

To estimate ocean heat content and associated thermosteric sea-level changes from 1950 to 2003 (see Methods), we use temperature data¹¹ from reversing thermometers (whole period), expendable bathy-thermographs (XBTs; since the late 1960s), modern and more accurate conductivity–temperature–depth (CTD) measurements from research ships (since the 1980s) and Argo floats (mostly from 2001). XBTs, providing more than 50% of the data, measure temperature from free-falling expendable probes at depths estimated from the elapsed time since release at the surface. Significant systematic biases in XBT temperatures⁹ are associated primarily with errors in the estimated depth of observations, probably a result of subtle differences in the manufacture of the XBTs⁸. We use a recent time-variable XBT fall-rate correction⁸ to minimize these biases. To recover the large-scale patterns from sparse temperature data, we use a reduced-space optimal interpolation technique⁵. This approach helps overcome the low bias in previous estimates of trends in heat content^{1,12} and sea level^{12,13}, particularly in the Southern Hemisphere^{3,14}, and provides rigorous error estimates (see Methods).

Near-globally averaged anomalies of ocean heat content in the upper 700 m and 100 m (plotted as three-year running means) and

sea surface temperature now track each other at multi-decadal time-scales (Fig. 1). These global averages all show a slight increase from 1950 to about 1960, a 15-year period to the mid-1970s of zero or slightly negative trend and, after the 1976–1977 climate shift, a steady rise to the end of the record. This pattern is also observed in thermosteric sea level (Fig. 2). Including time-variable error estimates, the linear trend in ocean heat content in the upper 700 m gives a total change of $16 \pm 3 \times 10^{22} \text{ J}$ from 1961 to 2003 (equivalent to an air–sea heat flux of $0.36 \pm 0.06 \text{ W m}^{-2}$ over the ocean surface area considered, $3.3 \times 10^{14} \text{ m}^2$; all error estimates quoted are one standard deviation), with about 91% stored in the upper 300 m. For thermosteric

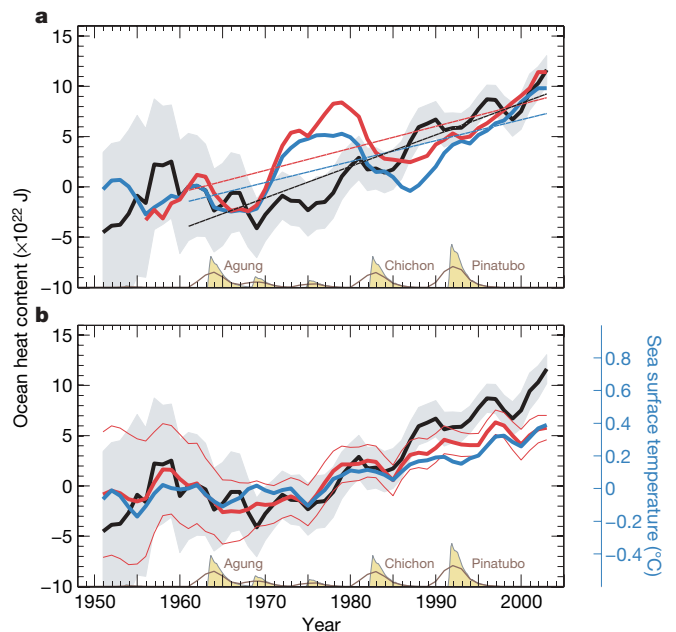


Figure 1 | Estimates of ocean heat content and sea surface temperature. **a**, Comparison of our upper-ocean heat content (black; grey shading indicates an estimate of one standard deviation error) with previous estimates (red¹ and blue¹²) for the upper 700 m. The straight lines are linear fits to the estimates. The global mean stratospheric optical depth³¹ (beige, arbitrary scale) at the bottom indicates the timing of major volcanic eruptions. The brown curve is a three-year running average of these values, included for comparison with the smoothed observations. **b**, Comparison of our 700-m (thick black line, as in **a**) and 100-m (thick red line; thin red lines indicate estimates of one standard deviation error) results with sea surface temperature³⁰ (blue; right-hand scale). All time series were smoothed with a three-year running average and are relative to 1961.

¹Centre for Australian Weather and Climate Research, CSIRO Marine and Atmospheric Research, GPO Box 1538, Hobart, Tasmania 7001, Australia. ²Antarctic Climate and Ecosystems Cooperative Research Centre, Hobart, Private Bag 80, Tasmania 7001, Australia. ³Program for Climate Model Diagnosis and Intercomparison, Lawrence Livermore National Laboratory, Mail Code L-103, 7000 East Avenue, Livermore, California 94550, USA.

sea level, the rise is about 22 mm (a trend of $0.52 \pm 0.08 \text{ mm yr}^{-1}$, with about 97% in the upper 300 m). These ocean warming and thermal expansion rates are more than 50% larger than previous estimates for the upper 300 m (refs 1, 13) and are about 50% larger for the upper 700 m (refs 1, 12, 13). Since 1976, the equivalent rates have been 0.40 W m^{-2} and 0.59 mm yr^{-1} , and for the period of the modern satellite altimeter record from 1993 to 2003 they have been 0.35 W m^{-2} and 0.79 mm yr^{-1} , less than previous estimates¹⁵, which were biased high by errors in the fall rate of XBTs^{8–10}. Exclusion of the XBT data from the reconstructions produces equivalent trends but with larger uncertainties because of the reduced spatial coverage.

Our time series of heat content and thermosteric sea level (Figs 1, 2) now show little indication of the large spurious rise in the early 1970s and the subsequent decrease in the early 1980s (about $6 \times 10^{22} \text{ J}$ and about 10 mm), which dominate previous estimates^{1,12,13} and were largely the result of instrumental biases⁸. This result is confirmed if we remove the XBT data from the reconstructions. However, there are smaller variations in heat content (less than $3 \times 10^{22} \text{ J}$) and thermosteric sea level (less than 5 mm), roughly consistent in both amplitude and timing with the impact of volcanic eruptions in 1963, 1982 and 1991 (refs 16–18).

We compare our estimates for the upper 300 m (not shown) and 700 m (Fig. 2) with equivalent values from simulations of the twentieth century in the World Climate Research Programme's Coupled Model Intercomparison Project Phase 3 (WCRP CMIP-3) conducted in support of the Intergovernmental Panel on Climate Change Fourth Assessment Report (IPCC AR4). The CMIP-3 simulations examined here are summarized in Supplementary Information. For models that do not include volcanic (stratospheric) aerosols, the changes in simulated ocean heat content and thermosteric sea level have smaller decadal variability than the observations and larger long-term trends (Fig. 2a, b).

For simulations with volcanic forcing (but excluding two models, one that simulates the volcanic forcing by adjusting the solar constant (pale green diamond), and one that responds more strongly to the

Agung eruption (orange circle) than the other models¹⁷), the observed and modelled heat content and thermal expansion time series are similar, with comparable falls in heat content and sea level after volcanic eruptions (Fig. 2c, d). After removal of a linear trend for 1961–1999, the average of the model variances is marginally larger than the variance of the (smoothed) observed time series (which also contains observational uncertainty). The simulated and the observed time series are correlated at zero lag (average correlation coefficient of 0.60). The magnitude of these simulated responses varies because of differences in model physics and estimated volcanic forcings^{16–18}. In addition, there are significant differences between ensemble members of the same model.

From 1961 to 1999, the simulations with volcanic forcing have multi-decadal trends in heat storage and thermosteric sea-level rise substantially smaller than those without volcanic forcing. The model trends with volcanic forcing are closer to the observations but are on average about 28% smaller in the upper 300 m and about 10% smaller in the upper 700 m; that is, 73% of the heat storage in the models is in the upper 300 m, in contrast with 93% in the observations.

We combine our estimates of thermosteric sea level with estimates of thermal expansion in the deep ocean and of the increased mass of the ocean in an attempt to balance the sea-level budget (Fig. 3). Although observations and models confirm that recent warming is greatest in the upper ocean, there are widespread observations of warming deeper than 700 m (refs 19–21). The only global observational estimate of thermal expansion in the deep ocean¹³ indicates that integrating to 3,000 m gives a 20% increase on the value for the upper 700 m (or 0.07 mm yr^{-1}). This value is probably underestimated because of the use of standard optimal interpolation techniques and the sparse deep observational database, particularly in the Southern Hemisphere¹⁴. In the ocean reanalysis from the German Consortium for Estimating the Circulation and Climate of the Ocean model, the 1962–2001 ocean thermal expansion was about 0.6 mm yr^{-1} in the upper 700 m, with an additional 50% (about 0.3 mm yr^{-1}) from the ocean below 700 m (ref. 22). For estimating

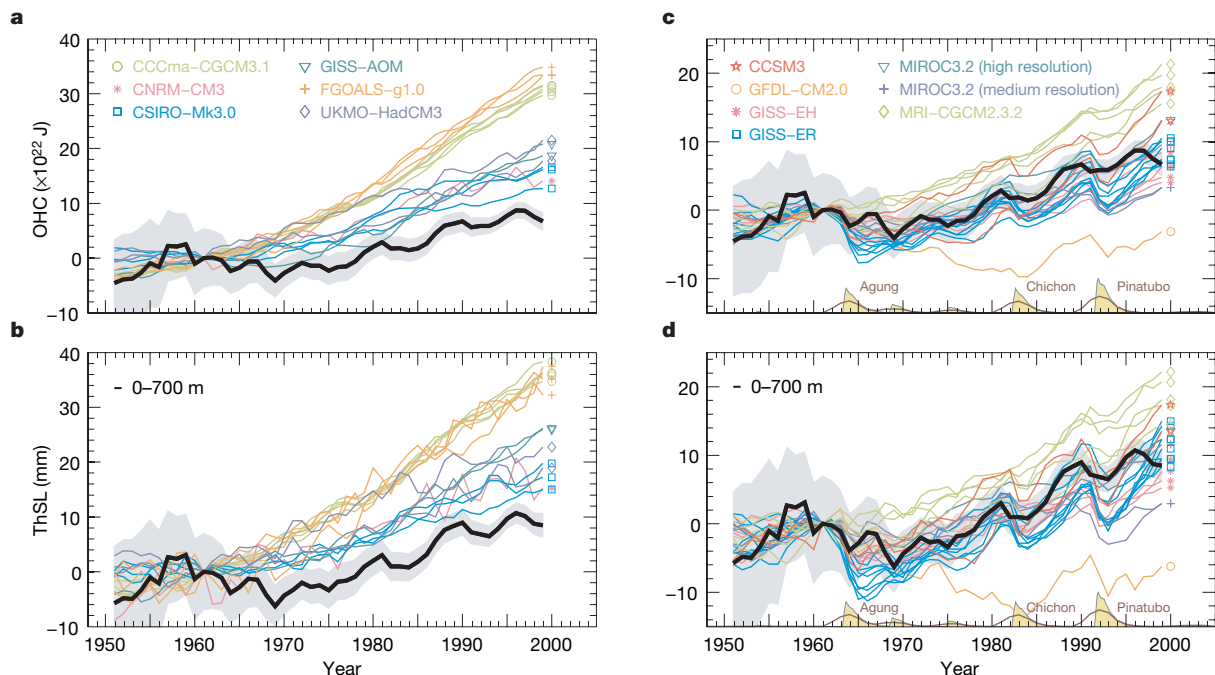


Figure 2 | Comparison of observed and simulated ocean heat content (OHC) and thermosteric sea level (ThSL) estimates for the upper 700 m. **a, b**, Models without volcanic forcing. **c, d**, Models with volcanic forcing. The observations are smoothed as in Fig. 1 and the model results are yearly averages. All models include greenhouse gas and tropospheric aerosol forcings. See Supplementary Information for more details of the models and

the climatic forcings. The stratospheric aerosol loadings³¹ of the major volcanic eruptions are shown at the bottom of **c** and **d**. The brown curve is a three-year running average of these values, included for comparison with the smoothed observations. The grey shading indicates estimates of one standard deviation error for the observed time series, and all time series are relative to 1961.

the sea-level budget we use a deep-ocean thermal expansion of $0.2 \pm 0.1 \text{ mm yr}^{-1}$ (Fig. 3a) but recognize that this value is uncertain. This thermal expansion rate implies additional heat storage of about $8 \times 10^{22} \text{ J}$ (0.2 W m^{-2}) in the deep ocean.

For 1961–2003, glaciers and ice caps contribute $0.5 \pm 0.2 \text{ mm yr}^{-1}$ to global sea-level rise (Fig. 3a), increasing to $0.8 \pm 0.2 \text{ mm yr}^{-1}$ for 1993–2003 (ref. 23). For 1993–2003, the estimated contributions for the Greenland and Antarctic ice sheets are 0.21 ± 0.07 and $0.21 \pm 0.35 \text{ mm yr}^{-1}$, respectively². There is little information to constrain ice sheet contributions for previous decades, but it is thought that the Greenland contribution has increased significantly in recent years²⁴. We use a contribution that increases linearly from zero in 1961 to the 1990s value. The Antarctic ice sheet is thought to be still responding to changes since the last glacial maximum¹⁹. These long timescales suggest that there may have been little change in the Antarctic contribution since 1961.

Hydrological models indicate decadal changes in terrestrial water storage but little long-term trend²⁵ (Fig. 3a). Terrestrial storage associated with multi-decadal human interference in the water system is poorly determined. The two largest terms, the building of dams (about 0.55 mm yr^{-1} over the past half century²⁶) and the mining of groundwater¹⁹, are likely to be of similar size but of opposite sign. For this reason we have not included these terms in Fig. 3.

We update *in situ* estimates of globally averaged sea level by applying established techniques^{6,7}, but using empirical orthogonal functions determined from a longer set of altimeter data (1993–2006), using a larger number of tide gauges than in previous studies and

correcting the tide-gauge data for the impact of atmospheric pressure²⁷, as well as glacial isostatic adjustment. The globally averaged sea-level trend from this new estimate and one using an independent technique²⁸ are almost identical from 1961 to 2003, with a trend of $1.6 \pm 0.2 \text{ mm yr}^{-1}$ (Fig. 3b). The sum of contributions to sea-level rise is $1.5 \pm 0.4 \text{ mm yr}^{-1}$, not significantly different from the estimated value. The almost exact agreement in 2003 is fortuitous and the different decadal variability is an indication of the uncertainty in the estimates and the (unknown) variability in the cryospheric and deep-ocean contributions. From 1993 to 2003, the sum of contributions is 2.4 mm yr^{-1} , again almost equal to the estimated trend from tide gauges of 2.3 mm yr^{-1} and still in the upper quartile of the IPCC projections from 1990 (ref. 29). Note that the sea level estimated from satellite altimeter observations follows the *in situ* estimate closely up to 1999 and then begins to diverge, implying a higher rate of rise. It is unclear why the *in situ* and satellite estimates diverge, and careful comparison is urgently needed.

The improved closure of the sea-level budget over multi-decadal periods (Fig. 3b) and the better agreement in the magnitude of observed and simulated decadal variability (Fig. 2c, d) increase confidence in the present results and represent progress since the last two IPCC reports^{2,19}. The results indicate an ongoing need for careful quality control of observational data and also for detailed global and regional comparisons of observational estimates with climate models to understand the implications for the detection, attribution and projection of climate change and sea-level rise.

METHODS SUMMARY

We reconstructed near-global monthly thermosteric sea level anomalies for 1950–2003 and for different depth levels (100, 200, 300, 400, 500 and 700 m), using a reduced-space optimal interpolation technique⁶. This technique is designed to recover the large-scale robust patterns that can be derived from sparse data and has previously been used to estimate global sea surface temperature³⁰, atmospheric pressure²⁷ and sea level^{6,7}. The globally averaged time series were computed with equal-area weighting. We converted the thermosteric sea-level fields into changes in ocean heat content using a spatially variable regression. Because of the sparse spatial coverage, particularly in the earlier part of the period, the monthly reconstructed fields contained substantial noise that were reduced by forming three-year running means.

Full Methods and any associated references are available in the online version of the paper at www.nature.com/nature.

Received 27 December 2007; accepted 3 May 2008.

- Levitus, S., Antonov, J. & Boyer, T. T. Warming of the world ocean, 1955–2003. *Geophys. Res. Lett.* **32**, L02604, doi:10.1029/2004GL021592 (2005).
- Bindoff, N. L. *et al.* in *Climate Change 2007: The Physical Science Basis. Contribution of Working Group I to the Fourth Assessment Report of the Intergovernmental Panel on Climate Change* (eds Solomon, S. *et al.*) 385–432 (Intergovernmental Panel on Climate Change, Cambridge, 2007).
- Gregory, J. M., Banks, H. T., Stott, P. A., Lowe, J. A. & Palmer, M. D. Simulated and observed decadal variability in ocean heat content. *Geophys. Res. Lett.* **31**, L15312, doi:10.1029/2004GL02058 (2004).
- AchutaRao, K. M. *et al.* Simulated and observed variability in ocean temperature and heat content. *Proc. Natl Acad. Sci. USA* **204**, 10768–10773 (2007).
- Kaplan, A., Kushnir, Y. & Cane, M. A. Reduced space optimal interpolation of historical marine sea level pressure. *J. Clim.* **13**, 2987–3002 (2000).
- Church, J. A., White, N. J., Coleman, R., Lambeck, K. & Mitrovica, J. X. Estimates of the regional distribution of sea-level rise over the 1950 to 2000 period. *J. Clim.* **17**, 2609–2625 (2004).
- Church, J. A. & White, N. J. A 20th century acceleration in global sea-level rise. *Geophys. Res. Lett.* **33**, L01602, doi:10.1029/2005GL024826 (2006).
- Wijffels, S. E. *et al.* Changing expendable bathythermograph fall-rates and their impact on estimates of thermosteric sea level rise. *J. Clim.* doi:10.1175/2008JCLI2290.1 (in the press).
- Gouretski, V. & Koltermann, K. P. How much is the ocean really warming? *Geophys. Res. Lett.* **34**, L01610, doi:10.1029/2006GL027834 (2007).
- Willis, J., Lyman, J. M., Johnson, G. C. & Gilson, J. Correction to 'Recent cooling of the upper ocean'. *Geophys. Res. Lett.* **34**, L16601, doi:10.1029/2007GL030323 (2007).
- Ingleby, B. & Huddleston, M. Quality control of ocean temperature and salinity profiles—historical and real time data. *J. Mar. Syst.* **65**, 158–175 (2007).
- Ishii, M., Kimoto, M., Sakamoto, K. & Iwasaki, S.-I. Steric sea level changes estimated from historical ocean subsurface temperature and salinity analyses. *J. Oceanogr.* **62**, 155–170 (2006).

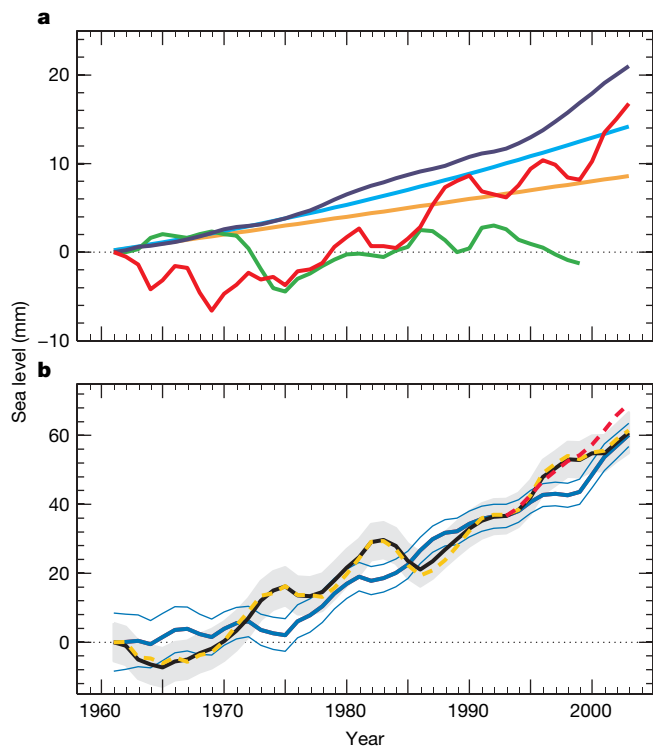


Figure 3 | Total observed sea-level rise and its components. **a**, The components are thermal expansion in the upper 700 m (red), thermal expansion in the deep ocean (orange), the ice sheets of Antarctica and Greenland (cyan), glaciers and ice caps (dark blue) and terrestrial storage (green). **b**, The estimated sea levels are indicated by the black line (this study), the yellow dotted line²⁸ and the red dotted line (from satellite altimeter observations). The sum of the contributions is shown by the blue line. Estimates of one standard deviation error for the sea level are indicated by the grey shading. For the sum of components, we include our rigorous estimates of one standard deviation error for upper-ocean thermal expansion; these are shown by the thin blue lines. All time series were smoothed with a three-year running average and are relative to 1961.

13. Antonov, J. I., Levitus, S. & Boyer, T. P. Thermohaline sea level rise, 1955–2003. *Geophys. Res. Lett.* **32**, L12602, doi:10.1029/2005GL023112 (2005).
14. Gille, S. T. Decadal-scale temperature trends in the Southern Hemisphere ocean. *J. Clim.* **10.1175/2008JCLI2131.1** (in the press).
15. Willis, J., Roemmich, D. & Cornuelle, B. Interannual variability in upper-ocean heat content, temperature and thermohaline expansion on global scales. *J. Geophys. Res.* **109**, C12037, doi:10.1029/2003JC002260 (2004).
16. Church, J. A., White, N. J. & Arblaster, J. M. Significant decadal-scale impact of volcanic eruptions on sea level and ocean heat content. *Nature* **438**, 74–77 (2005).
17. Gleckler, P. J. *et al.* Krakatoa lives: The effect of volcanic eruptions on ocean heat content and thermal expansion. *Geophys. Res. Lett.* **33**, L17702, doi:10.1029/2006GL026771 (2006).
18. Delworth, T. L., Ramaswamy, V. & Stenchikov, G. L. The impact of aerosols on simulated ocean temperature, heat content, and sea level in the 20th century. *Geophys. Res. Lett.* **32**, L24709, doi:10.1029/2005GL024457 (2005).
19. Church, J. A. *et al.* in *Climate Change 2001: The Scientific Basis. Contribution of Working Group I to the Third Assessment Report of the Intergovernmental Panel on Climate Change* (eds Houghton, J. T. *et al.*) 639–693 (Cambridge Univ. Press, Cambridge, 2001).
20. Johnson, G. C. & Doney, S. C. Recent western South Atlantic bottom water warming. *Geophys. Res. Lett.* **33**, L14614, doi:10.1029/2006GL026769 (2006).
21. Johnson, G. C., Mecking, S., Sloyan, B. M. & Wijffels, S. E. Recent bottom water warming in the Pacific Ocean. *J. Clim.* **13**, 2987–3002 (2007).
22. Köhl, A., Stammer, D. D. & Cournelle, B. Interannual to decadal changes in the ECCO Global Synthesis. *J. Phys. Oceanogr.* **37**, 313–337 (2007).
23. Dyurgerov, M. B. & Meier, M. F. *Glaciers and the Changing Earth System: A 2004 Snapshot* (Occasional Paper 58, Institute of Arctic and Alpine Research, Univ. of Colorado, 2005).
24. Lemke, P. *et al.* in *Climate Change 2007: The Physical Science Basis. Contribution of Working Group I to the Fourth Assessment Report of the Intergovernmental Panel on Climate Change* (eds Solomon, S. *et al.*) 337–383 (Intergovernmental Panel on Climate Change, Cambridge, 2007).
25. Ngo-Duc, T., Laval, K., Polcher, J., Lombard, A. & Cazenave, A. Effects of land water storage on global mean sea level over the past half century. *Geophys. Res. Lett.* **32**, 9704–9707 (2005).
26. Chao, B. F., Wu, Y. H. & Li, Y. S. Impact of artificial reservoir water impoundment on global sea level. *Science* **320**, 212–214 (2008).
27. Allan, R. & Ansell, T. J. A new globally complete monthly historical mean sea level pressure dataset (HadSLP2): 1850–2004. *J. Clim.* **19**, 5816–5842 (2006).
28. Jevrejeva, S., Grinsted, A., Moore, J. C. & Holgate, S. J. Nonlinear trends and multiyear cycles in sea level records. *J. Geophys. Res.* **111**, C09012, doi:10.1029/2005JC003229 (2006).
29. Rahmstorf, S. *et al.* Recent climate observations compared to projections. *Science* **316**, 709, doi:10.1126/science.1136843 (2006).
30. Rayner, N. *et al.* Global analyses of sea surface temperature, sea ice, and night marine air temperature since the late nineteenth century. *J. Geophys. Res.* **108**, 4407, doi:10.1029/2002JD002670 (2003).
31. Ammann, C. M., Meehl, G. A. & Washington, W. M. A monthly and latitudinally varying volcanic forcing dataset in simulations of the 20th century climate. *Geophys. Res. Lett.* **30**, 16257, doi:10.1029/2003GL016875 (2003).

Supplementary Information is linked to the online version of the paper at www.nature.com/nature.

Acknowledgements This paper is a contribution to the Commonwealth Scientific Industrial Research Organization (CSIRO) Climate Change Research Program and Wealth from Oceans Flagship and was supported by the Australian Government's Cooperative Research Centres Programme through the Antarctic Climate and Ecosystems Cooperative Research Centre. C.M.D., J.A.C., N.J.W. and S.E.W. were partly funded by the Australian Climate Change Science Program. We acknowledge the modelling groups, the Program for Climate Model Diagnosis and Intercomparison (PCMDI) and the WCRP's Working Group on Coupled Modelling (WGCM) for their roles in making available the WCRP CMIP-3 multi-model data set. Support for P.J.G. and this data set at the Lawrence Livermore National Laboratory was provided by the Office of Science, US Department of Energy. The Centre for Australian Weather and Climate Research is a partnership between CSIRO and the Australian Bureau of Meteorology.

Author Contributions C.M.D. completed the analysis to determine the changes in ocean heat content and thermohaline sea-level rise and shared responsibility for writing the manuscript. J.A.C. conceived the study, directed the analysis and shared responsibility for writing the manuscript. N.J.W. completed the analysis of the sea-level data and provided the software for the sea-level and thermohaline sea-level reconstructions. P.J.G. analysed the model results. S.E.W. provided the corrections for the XBT data and the climatology, and made valuable comments. P.M.B. provided the pressure corrections to the Argo data. J.R.D. quality-controlled the Argo data. All authors contributed to the final version of the manuscript.

Author Information Reprints and permissions information is available at www.nature.com/reprints. Correspondence and requests for materials should be addressed to C.M.D. (catia.domingues@csiro.au).

METHODS

Ocean temperature data. To estimate ocean heat content for the upper 300 m and 700 m and the associated thermosteric sea level from 1950 to 2003, we used about 2.3 and 1.8 million profiles (shallow and deep, respectively) from the available 6 million ocean temperature profiles in the ENACT/ENSEMBLES version 3 (hereafter EN3) data set¹¹. We discarded profiles (about 1.7 million) that had bad quality flags, had coarse vertical resolution, were shallower than 100 m depth or were from higher latitudes than 65° N and 65° S. We carefully selected only the temperature profiles that were clearly identified and measured by XBTs (about 1.2 million and 1.0 million), for which we could apply a correction for the systematic errors⁸, bottles (about 1.1 million) and CTDs (about 700,000). We did not include temperature profiles from the remaining instrument types (1.8 million profiles, of which about 1.2 million are from Mechanical Bathymographs (MBTs)) because of a lack of understanding of their potential systematic biases⁸. To complement the XBTs, bottles and CTDs from the EN3 data set, we used the most recent version of our own quality-controlled Argo profiling floats (about 60,000), including corrections for pressure-sensor drift.

Temperature climatology. We produced a climatology from the observations by using a technique developed previously³², which includes spatially dependent terms and annual, semi-annual and linear trend terms at each grid point. We believe this is superior to most other available climatologies in which all years are simply averaged together, yielding young median observation dates in the Southern Hemisphere and old median dates in the data-rich areas of the Northern Hemisphere. Attempts to resolve more than a linear trend in time were also considered, but estimates were poorly constrained by the data.

Thermosteric sea level and ocean heat content. We converted temperature profiles into thermosteric sea level and ocean heat content relative to a number of fixed-depth reference levels, assuming climatological salinities from the World Ocean Atlas³³. We calculated anomalies relative to their monthly mean fields and binned them to a 1 month \times 1° \times 1° grid for the ice-free ocean equatorward of 65° N and 65° S. Our deepest calculation was performed with respect to 700 m, for comparison with earlier results^{1,12,13} and because many XBTs measure to this depth⁸. To take advantage of the greater number of observations in the upper ocean, the 0–700-m estimates are a sum of two depth integrations, 0–300 m and 300–700 m.

Reconstruction details. In our reconstruction we used the sparse but relatively long record of thermosteric sea-level anomalies to determine monthly amplitudes of the leading 30 empirical orthogonal functions (EOFs). The EOFs were used to model variability of the time-varying sea level and were calculated from 14 years (1993–2006) of satellite altimeter data. An additional constant (essentially a spatially uniform field) was included in the reconstruction to represent changes in the global mean^{6,7}. Before computing the EOFs, we applied an inverted barometer correction and removed annual and semi-annual signals as well as a globally averaged sea-level trend from the altimeter data.

Error estimates. The reduced-space optimal interpolation formalism⁵ provides estimates of errors on the basis of the data distribution and uncertainties in the hydrographic observations (instrumental and geophysical errors) as well as ocean eddy variability determined from satellite altimeter data. The latter two were combined in quadrature. The formal error estimates quoted in the text are for one standard deviation.

Systematic error corrections. We have significantly reduced the systematic biases present in previous analyses by eliminating data sets with unknown errors (for example MBTs), correcting the XBT fall-rate errors and by using the reduced-space optimal interpolation technique. Further refinements in identifying and correcting XBT errors may be possible in the future⁸ but it is likely that more than 70% of the earlier XBT biases have been corrected in this analysis. Further corrections are a complex issue that is currently being addressed by an international working group.

Ocean heat content regression. We converted the reconstructed near-global monthly maps of thermosteric sea level into ocean heat content maps by using coefficients obtained from a spatially variable linear regression between estimates of ocean heat content and thermosteric sea level. The regressions are calculated from the temperature profiles in 10° \times 10° grid boxes (following the World Meteorological Organization squares). The resultant correlation coefficients are at least 0.99.

32. Alory, G., Wijffels, S. & Meyers, G. M. Observed temperature trends in the Indian Ocean over 1960–1999 and associated mechanisms. *Geophys. Res. Lett.* 34, L02606 10.1029/2006GL028044 (2007).

33. Conkright, M. E. et al. *World Ocean Atlas 2001: Objective Analyses, Data Statistics, and Figures, CD-ROM Documentation* (National Oceanographic Data Center, Silver Spring, MD, 2002).